Bull. Mater. Sci. (2018) 41:41
https://doi.org/10.1007/s12034-018-1576-4

Properties of ternary NiFeW alloy coating by jet electrodeposition

J K YU[1,*], J ZHAO[1], M Q YU[2], H L LUO[2,3], Q QIAO[1], S ZHAI[1], Z F XU[2] and KAZUHIRO MATSUGI[2]

[1]State Key Laboratory of Metastable Materials Science and Technology, Yanshan University, Qinhuangdao 066004, People's Republic of China
[2]Graduate School of Engineering, Hiroshima University, 1-4-1, Kagamiyama, Higashi-Hiroshima 739-8527, Japan
[3]Hebei Provincial Key Laboratory of Heavy Machinery Fluid Power Transmission and Control, Yanshan University, Qinhuangdao 066004, People's Republic of China
*Author for correspondence (yujinku@ysu.edu.cn)

MS received 18 May 2017; accepted 1 September 2017; published online 23 March 2018

Abstract. In this paper, ternary NiFeW alloy coatings were prepared by jet electrodeposition, and the effects of lord salt concentration, jet speed, current density and temperature on the properties of the coatings, including the composition, microhardness, surface morphology, structure and corrosion resistance, were investigated. Results reveal that the deposition rate reaches a maximum value of 27.30 μm h^{-1}, and the total current efficiency is above 85%. The maximum microhardness is 605 HV, and the wear and corrosion resistance values of the alloy coating are good. Moreover, the ternary NiFeW alloy coating is smooth and bright, and it presents a dense cellular growth. The alloy plating is nanocrystalline and has face-centered cubic structure.

Keywords. Jet electrodeposition; NiFeW alloy coating; current efficiency; microstructure; microhardness.

1. Introduction

Interest in the electrodeposition of NiFeW ternary alloys has increased rapidly in recent years because of their excellent properties, such as physical, chemical and mechanical properties. The introduction of tungsten into NiFe alloy coatings improves their microhardness [1–6], wear resistance [5–7], corrosion resistance [8–10] and uniformity organization [11–14]. There are many studies about the excellent properties of FeW and NiW alloy coatings [15–19]. Ternary NiFeW alloy coatings may exhibit the excellent properties of the FeW and NiW alloy coatings, while eliminating the unwanted properties of the binary alloy coatings [20–24]. However, systematic researches on the electrodeposition of the NiFeW alloy coatings are yet to be conducted [4,23]. Zhan *et al* [23] and Donten *et al* [4] have conducted several experiments on the effects of various concentrations of electrolyte and electroplating parameters on the compositions and appearances of the NiFeW alloy coatings. However, the properties and microstructure of these deposits were scarcely studied.

In the present study, NiFeW alloy coatings were prepared through jet electrodeposition from an environmentally friendly electrolyte. The composition of the NiFeW alloy coatings can be controlled by adjusting the process parameters and electrolyte components. Their structure and properties such as microhardness, wear resistance and corrosion resistance were studied in detail and compared systematically. The optimized process conditions of electroplating NiFeW alloy were proposed.

2. Experimental

To ensure the surface quality of the copper plate substrate, we used a 13 mm × 13 mm industrial pure copper plate as the substrate and performed the following pretreatments before plating. The substrate was first immersed in a mixed solution of 270 g l^{-1} sulphuric acid and 40 g l^{-1} hydrochloric acid mixed solution to remove the pure copper oxide on the surface. Then, the copper plate was immersed in a 5 g l^{-1} of NaOH, 5 g l^{-1} of Na_2CO_3, 10 g l^{-1} of Na_3PO_4 and 1 ml l^{-1} of OP-10 mixed solution to remove cutting oils, washed in 60–70°C hot water and cold water, respectively, weakly etched in a 10% $Ni(NH_2SO_3)_2 \cdot 4H_2O$ solution for 10 min, and finally washed with deionized water.

The following chemicals were used: $Na_2WO_4 \cdot 2H_2O$ (40 g l^{-1}), $Ni(NH_2SO_3)_2 \cdot 4H_2O$ (300 g l^{-1}), $FeCl_2 \cdot 4H_2O$ (3 g l^{-1}), $NiCl_2 \cdot 4H_2O$ (5 g l^{-1}), $Na_3C_6H_5O_7 \cdot 2H_2O$ (40 g l^{-1}), H_3BO_3 (40 g l^{-1}), sodium dodecyl sulfate (as a wetting agent, 0.02 g l^{-1}), saccharin (as stress removal agent and brighteners, 5 g l^{-1}) and ascorbic acid (V_c as stabilizer, 3 g l^{-1}). A current density (D_K) of 10–200 A dm^{-2}, a pH value

J K Yu conceived the project. J Zhao, M Q Yu, H L Luo and S Zhai designed the experiments.

of 3.8–4.2, a temperature of 50–65°C, jet speed of 0–5 m s^{-1} and a copper sheet (as the cathode material) were used for plating. Analytical reagents and deionized water were used for the plating bath, where 5 g l^{-1} of NaOH or 10 g l^{-1} of $Ni(NH_2SO_3)_2 \cdot 4H_2O$ was used to control the pH value.

A HS-4800 field scanning electron microscope (FSEM) (Hitachi, East Coast Port City, Honshu Island) attached with an INC250 spectrometer (energy dispersive spectroscopy (EDS)) was used to analyse the morphology and Ni, Fe and W contents of NiFeW alloy coatings. A FM-ARS9000 hardness tester was used to measure the hardness of the NiFeW alloy coatings. The applied force and time were 50 *g* and 15 s, respectively. The hardness value was obtained from the average value of hardness from five measurements.

The deposition rate is characterized by the coating thickness difference method. The thickness of the samples before and after electrodeposition was measured by using a micrometer. Before every thickness measurement, the samples were cleaned with ethanol and dried completely. The coating deposition rate was obtained by dividing the thickness difference by the electrodeposition time. The deposition rate was obtained by computing the average value of the five measurements.

A CHI660A electrochemical workstation was used to measure the polarization curves to derive the corrosion resistance of the alloy coatings in a 3.5 wt% NaCl solution. A three-electrode cell, which comprises a NiFeW alloy coating as the working electrode, a platinum piece as the counter electrode and a saturated calomel electrode as the reference electrode, was used. The polarization curves were measured at an initial potential of −1.3 V, a final potential of 1.2 V and a scan rate of 10 mv s^{-1}.

The computing method of the current efficiency shown below is based on the analysis of the components of the ternary alloy membrane [24].

$$\eta = \frac{\sum_{i=1}^{n} G \times a_i \times k_i}{Q_{\text{total}}} \times 100\%,$$

where n is the number of components ($n = 3$), G is the total weight of coatings (g), a_i is ith percentage of components in the alloy and k_i is the ith electrochemical equivalent value of the components (Ah g^{-1}).

3. Results and discussion

In this work, NiFeW alloy coatings were prepared according to the optimal solution formula with different concentrations of $FeCl_2 \cdot 4H_2O$, $Na_2WO_4 \cdot 2H_2O$ and $Ni(NH_2SO_3)_2 \cdot 4H_2O$ in the plating bath. The process parameters were temperature (60°C), D_K (60 A dm^{-2}), jet speed (3 m s^{-1}) and pH value (4.0). The influence of the lord salt concentration on the NiFeW alloy coating contents and microhardness was investigated.

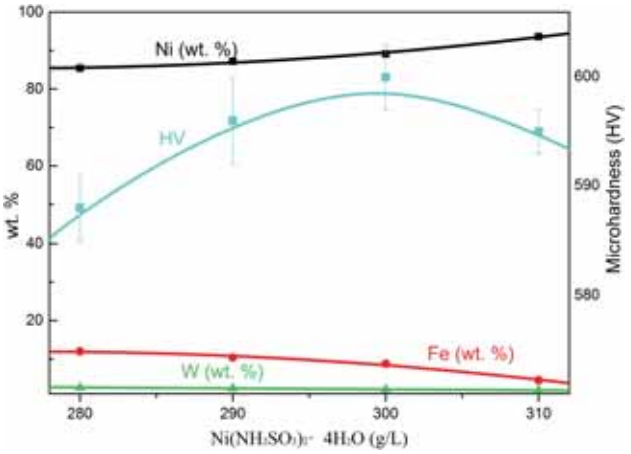

Figure 1. Composition and microhardness of the coating *vs*. $Ni(NH_2SO_3)_2$ concentration of the plating bath. The W and Fe contents decrease with the increasing $Ni(NH_2SO_3)_2 \cdot 4H_2O$ concentration in the plating bath. First, the microhardness increases and subsequently decreases with increasing $Ni(NH_2SO_3)_2 \cdot 4H_2O$ concentration in the plating bath.

The relation curve of the $Ni(NH_2SO_3)_2 \cdot 4H_2O$ concentration and the Fe and W content and the microhardness of NiFeW alloy coatings is shown in figure 1. The W and Fe contents in NiFeW alloy coatings decrease with the increase in the $Ni(NH_2SO_3)_2 \cdot 4H_2O$ concentration in the plating bath. The W content decreased from 2.60 to 1.90%, and the Fe content tend to decrease very quickly from 12.10 to 4.52% with the increase in the $Ni(NH_2SO_3)_2 \cdot 4H_2O$ concentration in the range of 280–310 g l^{-1}. In the electrodeposition process, Ni^{2+} concentration increases with increase in the $Ni(NH_2SO_3)_2 \cdot 4H_2O$ concentration in the plating bath, and it will increase the concentration of Ni^{2+} near the cathode, the proportion increases of hydrate Ni^{2+} in the deposition reaction, it prevents the deposition of Fe^{2+} and WO_4^{2-}. Thus, the Ni content in coatings increases and the W and Fe contents decrease.

The microhardness of the NiFeW alloy first increases, then decreases with the increase in the $Ni(NH_2SO_3)_2 \cdot 4H_2O$ concentration in the plating bath. A $Ni(NH_2SO_3)_2 \cdot 4H_2O$ concentration of 300 g l^{-1} and alloy coating maximum microhardness of 602 HV. The alloy coatings obeyed the direct Hall–Petch relation above a critical size, where the hardness increased with decrease in crystallite size and the inverse Hall–Petch relation below a critical size [13]. To guarantee the quality of the alloy coating and maintain the alloy coating deposition rate, the $Ni(NH_2SO_3)_2 \cdot 4H_2O$ concentration of 300 g l^{-1} was chosen.

Figure 2 shows the curve of the Na_2WO_4 concentration in the plating bath, and the microhardness and the W and Fe contents of the NiFeW alloy coatings. The figure shows that the Na_2WO_4 concentration in the plating bath does not affect the coating components significantly. Under certain conditions, the Fe^{2+} and Ni^{2+} concentrations in the plating bath remain the same, and the W content of NiFeW alloy coatings first

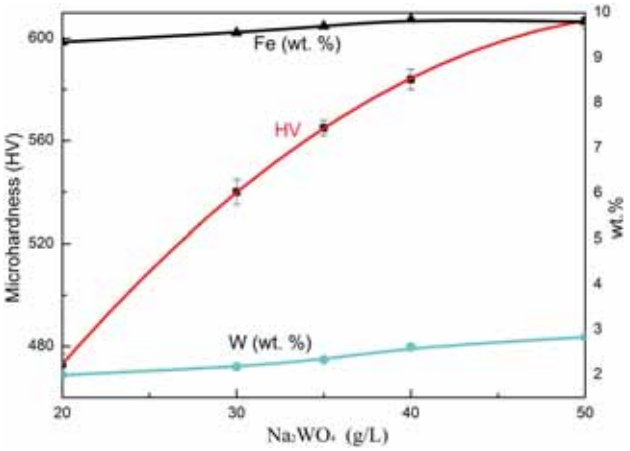

Figure 2. Microhardness and W and Fe contents of NiFeW alloy coatings *vs*. Na_2WO_4 concentration of the plating bath. The Fe and W contents increase with the increasing Na_2WO_4 concentration in the plating bath. The microhardness increases with increasing Na_2WO_4 concentration of the plating bath.

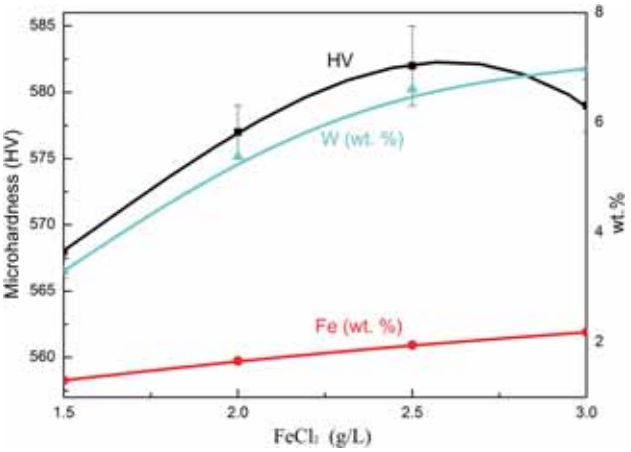

Figure 3. Microhardness and W and Fe contents of NiFeW alloy coatings *vs*. $FeCl_2$ concentration of the plating bath. The Fe and W contents increase with the increasing $FeCl_2$ concentration in the plating bath. First, the microhardness increases and subsequently decreases with the increasing $FeCl_2 \cdot 4H_2O$ concentration in the plating bath.

increases rapidly to a certain degree, then slows down with the increase in the Na_2WO_4 concentration. The changes in the Fe and W contents of NiFeW alloy coatings have the same trend. This shows that W and Fe deposits will interact. Under the process conditions, the W content of alloy coating reaches the maximum. After which, the W content of the alloy coating no longer increases as the Na_2WO_4 concentration of the plating bath increases. When the Na_2WO_4 concentration of the plating bath reaches more than 50 g l^{-1}, the Na_2WO_4 produces precipitation, and the W content of the alloy coatings increase slowly [23].

As shown in figure 2, the microhardness of the NiFeW alloy coatings was increased from 477 to 603 HV with the increase in the Na_2WO_4 concentration of the plating bath form 20 to 50 g l^{-1}, and the coating hardness value increased to 125 HV. This is attributed to the increase in the Na_2WO_4 concentration of the plating bath that results in the increase in the W contents of alloy coatings from 2 to 3%.

The relation curve of the $FeCl_2$ concentration in the plating bath and the microhardness and the W and Fe contents in the NiFeW alloy coatings is shown in figure 3. The W and Fe contents of the alloy coatings increase with the increase in the $FeCl_2$ concentration in the plating bath. The Fe content increased from 3.30 to 6.98%, and W content increased from 1.31 to 2.18% with the increase in the $FeCl_2$ concentration from 1.50 to 3.00 g l^{-1}. In the process of electrodeposition, the ionic strength of Fe^{2+} increases with the increase in the $FeCl_2$ concentration in the plating bath, and the Fe^{2+} concentration in cathode increases with the increase in the Fe^{2+} concentration in the plating bath, and this increase could promote the deposition of Fe^{2+}. Thus, the Fe content in coatings increases. The Fe^{2+} of the plating bath and the WO_4^{2-} induced co-deposition effect leads to the increase in the W content of the alloy coatings and the increase in the $FeCl_2$ concentration of the plating bath.

The microhardness of the NiFeW alloy first increases, then decreases with the increase in the $FeCl_2$ concentration of the plating bath. When the $FeCl_2$ concentration was 2.0 g l^{-1}, the maximum microhardness for NiFeW alloy coatings was 580 HV. The Fe content of the alloy coatings increases because the $FeCl_2$ concentration of the plating bath increases. Concurrently, the W content of the alloy coatings increases. Therefore, the microhardness of the alloy coatings increases.

The influence of jet speed (v) on the content, microhardness, surface topography and microstructure of NiFeW alloy coatings was studied under a bath temperature of 60°C and a D_K of 60 A dm^{-2}. The relation curve of v and the microhardness, and the W and Fe contents of the NiFeW alloy coatings are shown in figure 4. The W and Fe contents increase with the increase in v. The Fe content increased from 2.3 to 2.72% and the W content increased from 8.54 to 9.83% with the increase in v in the range of 0–5 m s^{-1}. Jet electrodeposition with a special power plant increases the moving velocity of metal ions; metal ions near the cathode are consumed, and the concentration polarization is reduced due to the slow ion migration.

In addition, as v increases, the thickness of the cathode surface and the diffusion layers decreases, and the metal ion concentration of the surface and the diffusion layers increase. During electrodeposition, Fe^{2+} is reduced more easily than Ni^{2+}, and Fe^{2+} is also preferably deposited. Thus, the Fe content of the NiFeW alloy coatings increases, and Fe^{2+} and WO_4^{2-} induce co-deposition. Consequently, the Fe and W contents of the alloy coatings increase with the increase in v.

The microhardness increases with the increase in v. When v was 3 m s^{-1}, the maximum microhardness of the alloy

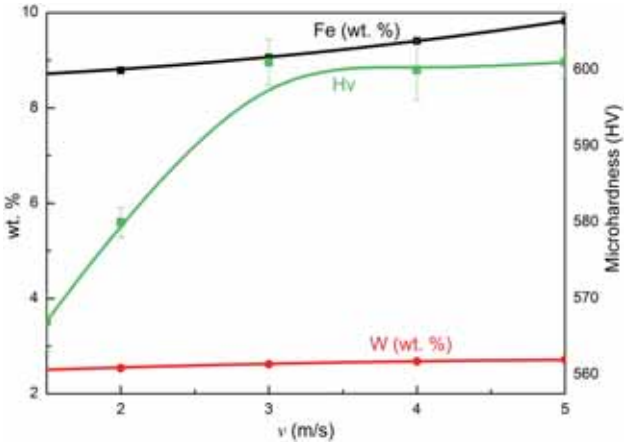

Figure 4. Microhardness and W and Fe contents of NiFeW alloy coatings *vs*. speed (v). Fe and W contents increase with the increasing v. The microhardness of NiFeW alloy coatings increases with increasing v value, reaches the maximum, and remains unchanged thereafter.

coating was 600 HV. This result can be explained by the decrease of the alloy coating grain size with the increasing v. Thereafter, the microhardness of the alloy coatings remains unchanged with the increasing v. Because of increase in the jet rate of the electrolyte, the concentration of ions increases in the deposition, the electrodeposition rate is accelerated, the grain size of alloy coating is reduced, and the hardness value of alloy coating increases. The alloy coatings obeyed the direct Hall–Petch relation. When jet rate of the electrolyte increases to a certain value, then the reaction speed no longer increases.

Figure 5 shows SEM images of the NiFeW alloy coatings at different v values. The NiFeW ternary alloy plating surface presents a granular structure by common electroplating preparation (figure 5a). With the increase in v of 1 m s^{-1}, the alloy coating shows granular and cellular structures (figure 5b). When v is 3 m s^{-1}, the alloy coating surface displays a fully formed cellular structure (figure 5c). Moreover, the cellular structure of the NiFeW ternary alloy coating surface is observed, when v continues to increase by 5 m s^{-1} (figure 5d). During crystal nucleus nucleation, low nucleation energy results in the high possibility of crystal nucleus formation, i.e., a high formation rate results in a fine crystalline grain size. In jet electrodeposition, the cathodic overpotential increases with the increase in v, thus, the nucleation rate increases, and the grain size is small [25]. There are two fundamental factors affecting grain size. They are rate of nucleation and crystal growth rate, when nucleation rate is greater than the growth rate of the nucleation, grain is refined. High cathode overpotential, high adsorption atomic number and low adsorption of atomic surface mobility were for a large number of nucleation, and inhibit the growth of grain. For jet electrodeposition, the cathode overpotential increases with jet velocity of the electrolyte increased, therefore, the

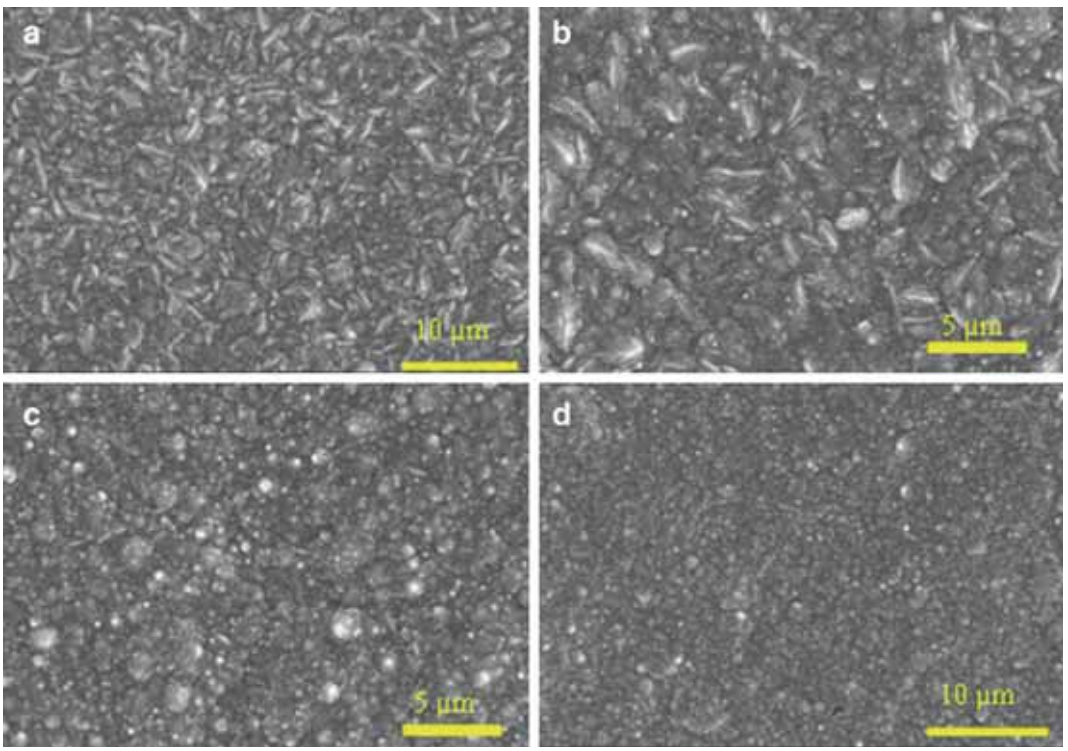

Figure 5. SEM images of the NiFeW alloy coatings in different v values: (**a**) 0, (**b**) 30, (**c**) 60 and (**d**) 120 m s^{-1}. The alloy coating surface topography changes from granular into cellular structure with increasing v values.

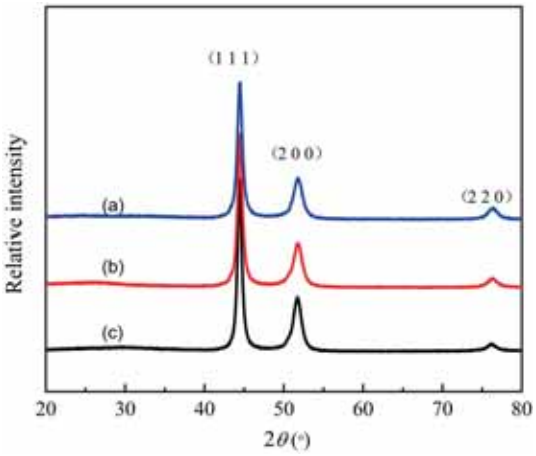

Figure 6. X-ray diffractometer patterns of the NiFeW alloy coatings with different v values: (**a**) 0, (**b**) 1.5 and (**c**) 3 m s^{-1}.

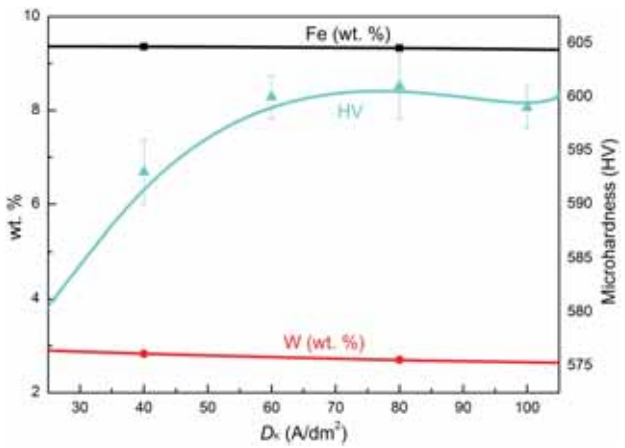

Figure 7. Microhardness and W and Fe contents of NiFeW alloy coatings *vs.* D_K. The Fe and W contents are essentially unchanged with the increasing D_K. The microhardness increases with increasing D_K, reaches the maximum, and remains unchanged thereafter.

nucleation probability increases. And greater speed, thinner diffuse layer, precipitates and adsorption of more hydrogen ions on the cathode surface were preventing the NiFeW nucleus to grew up. Spray this form to make additional energy to enter the liquid to provide nuclear power, promoting nucleation, and crystal dendrite can be broken to increase the number of nuclei, thus, causing the grain size to decrease.

The relation curve of jet speed (v) and microstructure of NiFeW alloy coatings is shown in figure 6, which indicates that the NiFeW ternary alloy coating is face-centered cubic structure. The (111) crystal orientation increases slightly with the increase in v. The alloy is made up of Ni-based solid solution and Ni_3 Fe. The atomic radius of Ni is smaller than that of Fe. To form the alloy coating, Ni atoms in the lattice original iron atoms will occupy the position and form Ni-based substitution solid solution; the radius difference between Ni and Fe changes the lattice constant and lattice distortion and hinders dislocation motion, thereby the grain refinement occurs [26].

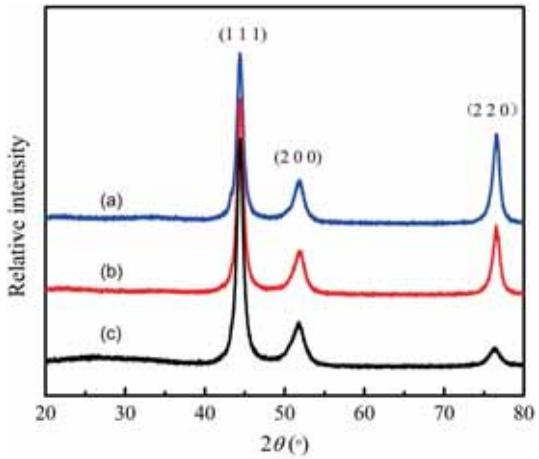

Figure 8. X-ray diffractometer patterns of the NiFeW alloy coatings with different D_K: (**a**) 10, (**b**) 40 and (**c**) 60 A dm^{-2}. With the increase in D_K, NiFeW alloy coating crystal orientation presents an apparent change from the initial (220) crystal orientation to (111).

Figure 7 shows the dependence of D_K on the microhardness and the W and Fe contents of the NiFeW alloy coatings. The W and Fe contents are essentially unchanged with increasing D_K. Evidently, D_K exerts no influence on the W and Fe contents of the alloy coatings; in NiFeW-induced co-deposition, determining the influence of alloy composition on electrolytic parameters is difficult [27].

The microhardness of the NiFeW alloy coatings increases with the D_K. When the D_K is 60 A dm^{-2}, the maximum microhardness of the alloy coating is 605 HV. Thereafter, the microhardness of alloy coatings remains unchanged.

The influence of D_K on the microstructure of the NiFeW alloy coatings was studied under a bath temperature of 60°C and v of 3 m s^{-1}. The results in figure 8 indicate that with increasing D_K, the NiFeW alloy coating crystal orientation presents an apparent change from the initial (220) crystal orientation to (111). Furthermore, the NiFeW ternary alloy coatings do not produce a new phase with the change in orientation.

The tribological tests of the alloy coating were evaluated using a MMU-5G end-face friction and wear testing machine (Jinan, China), which employed a load of 1–10 kN (force value relative error, ±1%), a rotational speed of 5–2000 r min^{-1} (error range, ±10 r min^{-1}), and a friction of 10–500 N (relative error of friction value, ±2%). The wear loss was calculated through the difference of the sample mass before and after the tribological tests. Each tribological test was repeated five times under the same conditions to reduce the artificial errors and obtain the standard deviations. The ϕ 40 mm coating samples with a polished surface were prepared through a wire cutting machine. The grinding material was 45# steel.

The experimental results are shown in table 1. The highest microhardness of the jet electrodeposition of the NiFeW ternary alloy plating is 605 HV. The erosion rate is lowest at 0.5734 g. Introducing W elements improves the microhardness and wear resistance of the alloy coating.

Table 1. Wear loss (g) of alloy coatings in the rotational speed of 100 r min^{-1}, load of 100 N and time of 20 min.

Alloy coatings	Microhardness (HV)	Wear loss (g)
NiFe	476	1.2210
NiFeW (ED)	562	0.7452
NiFeW (JD)	605	0.5734

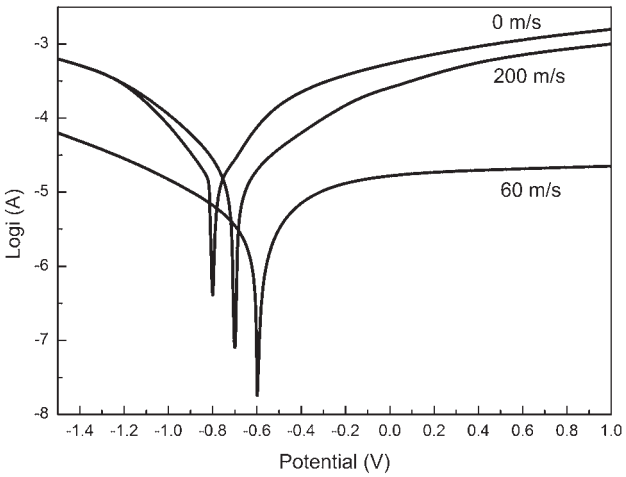

Figure 9. Cathodic polarization curves of the NiFeW alloy coatings with JED and ED.

Under the same experimental conditions, the friction and wear properties of alloy coatings and their hardness values are proportional. The increase in microhardness is helpful for the improvement of the alloy coating friction and wear performance [28].

Figure 9 shows the polarization curves of the NiFeW alloy coatings deposited using two different methods. The corrosion potential is −0.60 at the JED speed of 60 m s^{-1}, which is more positive than that using ED. With the JED and a voltage above −0.20 V, the current is almost constant with the increasing voltage. This result suggests that the coating surface is passivated, i.e., a passivated layer is formed on the surface of the coating. This passivated layer can prevent the further corrosion of the coating. Passivation also occurs at ∼ −0.2 V using the following set of parameters: 60°C, pH = 3, 4 A dm^{-2}, V_c = 3 g l^{-1} and ν = 60 m s^{-1}. Evidently, the coating deposited using JED exhibits the highest corrosion resistance, which is mainly attributed to the smooth and dense surface, the smallest grain size, the least impurities, and the fact that the Cl^- ions in the plating solution cannot easily penetrate coatings.

4. Conclusions

1. Preparation of the optimized formulation of the ternary alloy NiFeW: $Ni(NH_2SO_3)_2 \cdot 4H_2O$, 300 g l^{-1}; $Na_2WO_4 \cdot 2H_2O$, 40 g l^{-1}; $FeCl_2 \cdot 4H_2O$, 3.0 g l^{-1}; $NiCl_2 \cdot 4H_2O$, 5 g l^{-1}; $Na_3C_6H_5O_7 \cdot 2H_2O$, 40 g l^{-1}; H_3BO_3, 40 g l^{-1}; sodium dodecyl sulphate, 0.1 g l^{-1}; saccharin, 5 g l^{-1}; and ascorbic acid (V_c), 3 g l^{-1}.
2. Plating parameters: pH value of 4.0, D_K of 60 A dm^{-2}, temperature at 60°C, and jet speed of 4 m s^{-1}. Under the optimized formulation and technological conditions, the surface coating is uniform, bright and compact without obvious defects, and the coating possesses the crystalline NiFeW phase, which improves the performance of the copper substrate.
3. Under optimized formulation and technological conditions, the deposition rate is 27.3 μm min^{-1} and the current efficiency is above 85%.
4. Under optimized formulation and technological conditions, the maximum microhardness is 605 HV, and the wear and corrosion resistance values of the alloy coating are good.

Acknowledgements

We acknowledge the financial support from the Higher School of Science and Technology of Hebei Province in China (grant no. ZD2014055). This research work was also supported by the China Scholarship Council.

References

[1] Sriraman K R, Raman S G S and Seshadri S K 2007 *Mater. Sci. Eng. A* **460–461** 39
[2] Zelenovic L R, Cirovic N, Spasojevic M, Mitrovic N, Maricic A and Pavlovic V 2012 *Mater. Chem. Phys*. **135** 212
[3] Oliveira A L M, Costa J D, Sousa M B D, Alves J J N, Campos A R N, Santana R A C *et al* 2015 *J. Alloys Compd.* **619** 697
[4] Donten M, Cesiulis H and Stojek Z 2000 *Electrochim. Acta* **45** 3389
[5] Islam S H 2011 *Rare Met.* **30** 392
[6] He F J, Yang J, Lei T X and Gu C Y 2007 *Appl. Surf. Sci.* **253** 7591
[7] Chang L M, Wang Z T, Shi S Y and W Liu 2011 *J. Alloys Compd.* **509** 1501
[8] Wang S, Zeng C, Ling Y H, Wang J J and Xu G Y 2016 *Surf. Coat. Technol.* **286** 36
[9] Ji X L, Yan C Y, Duan H and Luo C Y 2016 *Surf. Coat. Technol.* **302** 208
[10] Kumar U P, Kennady C J and Zhou Q Y 2015 *Surf. Coat. Technol.* **283** 148
[11] Moussa S O, Ibrahim M A M and Rehim S S A E 2006 *J. Appl. Electrochem.* **36** 333
[12] Zhong Z M and Clouser S J 2014 *Surf. Coat. Technol.* **240** 380
[13] Sriraman K R, Raman S G S and Seshadri S K 2006 *Mater. Sci. Technol.* **22** 14
[14] He J, He F L, Li D W, Liu Y L and Yin D C 2016 *Colloids Surf. B* **142** 325

[15] Nagayama T, Yamamoto T and Nakamura T 2016 *Electrochim. Acta* **205** 178
[16] Matsui I, Mori H, Kawakatsu T, Takigawa Y, Uesugi T and Higashi K 2014 *Mater. Sci. Eng. A* **607** 505
[17] Yari S and Dehghanian C 2013 *Ceram. Int.* **39** 7759
[18] Elias L and Hegde A C 2015 *Surf. Coat. Technol.* **283** 61
[19] Zemanová M, Krivosudská M, Chovancová M and Jorík V 2011 *J. Appl. Electrochem.* **41** 1077
[20] Kiran U R, Kumar J, Kumar V, Sankaranarayana M, Nageswara Rao G V S and Nandy T K 2016 *Mater. Sci. Eng. A* **656** 256
[21] Hou K H and Chen Y C 2011 *Appl. Surf. Sci.* **257** 6340
[22] Spasojević M, Zelenović L R, Maričić A and Spasojević P 2014 *Powder Technol.* **254** 439
[23] Zhan H Q, He F J, Ju H and Zhao R S 2008 *J. Mater. Prot.* **41** 31
[24] Liu Y H and Yuan J M 1998 *J. Mater. Prot.* **31** 19
[25] Gu Z C and He L F 2010 *Plat. Finish.* **32** 1
[26] Meng Q P, Rong Y H and Xu Z Y 2002 *Sci. Chin.* (*Series E*) **32** 457
[27] Li H, He Y, He T, Qing D Y, Luo F J, Fan Y *et al* 2017 *J. Alloys Compd.* **704** 32
[28] Dong N, Zhang C L, Li J and Han P D 2016 *Rare Met. Mater. Eng.* **45** 0885